Editors' Suggestion

Impact of hyperfine contributions on the ground state of spin-ice compounds

J. Gronemann,[1] S. Chattopadhyay,[1,*] T. Gottschall,[1] E. Osmic,[1,2] A. T. M. N. Islam,[3] V. K. Anand,[3] B. Lake,[3,4] H. Kaneko,[5] H. Suzuki,[5] J. Wosnitza,[1,2] and T. Herrmannsdörfer[1]

[1]*Hochfeld-Magnetlabor Dresden (HLD-EMFL) and Würzburg-Dresden Cluster of Excellence ct.qmat, Helmholtz-Zentrum Dresden-Rossendorf, 01328 Dresden, Germany*

[2]*Institut für Festkörper- und Materialphysik, Technische Universität Dresden, 01062 Dresden, Germany*

[3]*Helmholtz-Zentrum Berlin für Materialien und Energie GmbH, 14109 Berlin, Germany*

[4]*Institut für Festkörperphysik, Technische Universität Berlin, 10623 Berlin, Germany*

[5]*Faculty of Mathematics and Physics, Kanazawa University, Kanazawa 920-1192, Japan*

(Received 25 August 2023; accepted 17 November 2023; published 14 December 2023)

We examined the magnetic ground state of the pyrochlore spin-ice compounds $Pr_2Hf_2O_7$ and $Ho_2Ti_2O_7$ by means of specific-heat, magnetization, and ac-susceptibility measurements in the mK regime. At these low temperatures, we observe an unexpected large specific heat and corresponding entropy, which diminish in applied magnetic fields. This evidences the presence of additional states beyond the electronic spin and orbital degrees of freedom. We can qualitatively explain the large specific heat by the coupling of the nuclear spins of ^{141}Pr and ^{165}Ho with their electronic counterparts, which leads to a complex hyperfine-coupled term scheme. With increasing fields, the nuclear and electronic spins decouple leaving only the electronic excitations in the measured temperature window. At intermediate fields, a rather evolved term scheme emerges that may explain the unusual hysteretic magnetization and a remarkable state with a negative magnetization found for $Ho_2Ti_2O_7$. Our findings bring deep insights to the complex ground state of pyrochlore spin-ice compounds and their low-energy excitations.

DOI: 10.1103/PhysRevB.108.214412

I. INTRODUCTION

The intricate balance and competition of magnetic interactions among the Ising-like spins in cubic pyrochlore oxides of the type $RE_2T_2O_7$, with RE being typically a rare-earth and T a transition-metal element, play a major role in the occurrence of their spectacular phenomena [1,2]. This includes, for example, the formation of spin ice accompanied by a residual ice entropy [3,4], magnetic-monopole excitations [5], all-in-all-out type antiferromagnetism accompanied by inverted hysteresis [6], as well as quantum-spin-liquid behavior [7]. A necessary condition to enable such a variety of exotic magnetic ground states is the presence of a large crystal-electric-field (CEF) splitting of strongly spin-orbit-coupled $4f$-electron states of the RE ions located on the pyrochlore lattice.

Due to this CEF splitting and the spin-orbit coupling, the combined electronic spin and orbital momentum can be described by a $J_{eff} = 1/2$ pseudospin [8,9]. Evidence for this ground-state doublet consisting of $|m_J = \pm J\rangle$ states exists, for example, in $Ho_2Ti_2O_7$ [10], while Pr-based pyrochlores reveal an additional small admixture of other $|m_J\rangle$ states [11,12]. In $Dy_2Ti_2O_7$, Ramirez *et al.* evidenced the spin-ice behavior of these doublets by the observation of a residual entropy in the specific heat [3]. Somewhat later, Pomaranski *et al.* reported that this spin-ice entropy is recovered over very long time scales [13]. High-field magnetization measurements on $Ho_2Ti_2O_7$ revealed the presence of Ising-type anisotropy of the moments formed by these pseudospins [14].

In this work, we show evidence that the magnetic ground states of pyrochlore compounds with enhanced hyperfine coupling are even more complex than discussed so far. This higher complexity arises in rare-earth-based systems, in which nuclear magnetic moments (such as those from ^{141}Pr and ^{165}Ho, both occurring with 100% natural abundance) contribute to the formation of hyperfine-coupled atomic quantum states. In non-Kramers rare-earth ions, indeed, hyperfine interaction with large electronic magnetic moments can give rise to enhanced nuclear magnetism [15,16].

In previous studies, μSR experiments revealed weak static magnetism that was taken as an indication for hyperfine-enhanced nuclear magnetism in $Pr_2Hf_2O_7$ [17]. Later, the enhanced interaction of the nuclear spin with its environment was attributed to the distortions of the lattice by the implanted muons [18]. Here, our thermodynamic measurements provide evidence for a considerably enhanced nuclear magnetism in two spin-ice materials even without invoking such lattice distortions.

Our investigations comprise extensive studies of the specific heat, ac susceptibility, and static magnetization of single-crystalline $Pr_2Hf_2O_7$ and $Ho_2Ti_2O_7$ samples. We focus on low temperatures between 0.05 and 20 K and magnetic fields up to 13 T, a regime where our study allowed us to obtain deep insights into the ground-state physics in these spin-ice materials. Our experimental results evidence that

*Present address: UGC-DAE Consortium for Scientific Research Mumbai Centre, 246-C CFB, BARC Campus, Mumbai 400085, India.

hyperfine contributions crucially modify the electronic magnetic ground-state doublet, which is an essential ingredient in the spin-ice behavior. At low temperatures, the nuclear spin $\vec{I}$ and the total angular momentum $\vec{J}$ couple to a combined angular momentum $\vec{F} = \vec{I} + \vec{J}$, leading to multiple-degenerate states described by the quantum number F.

II. EXPERIMENT

We performed the experiments on high-quality single-crystalline samples grown by the floating-zone technique at the Core Lab Quantum Materials, Helmholtz Zentrum Berlin für Materialien und Energie, Germany ($Pr_2Hf_2O_7$) and at Kanazawa University ($Ho_2Ti_2O_7$). The quality of the $Pr_2Hf_2O_7$ sample was established in Ref. [19], while the $Ho_2Ti_2O_7$ sample was previously reported in Ref. [14].

We measured the specific heat of both samples between 0.05 and 1 K using a dilution refrigerator and between 0.5 and 20 K in a ^{3}He cryostat. In both setups, we used the quasiadiabatic heat-pulse method by making use of a short heat pulse of defined power and observing the corresponding rise in temperature with high resolution. We extracted the magnetic contributions to the specific heat (C_{mag}) by subtracting the small lattice contributions; see dashed lines in Fig. 1(a). For that, we used our high-temperature data up to 40 K and fitted a T^3 plus T^5 term to them. Indeed, the phonon contribution only plays a role above about 5 K reaching about 50% of the total specific heat at 10 K. We calculated the magnetic-entropy change between T_1 and T using $\Delta S = \int_{T_1}^{T} \frac{C_{\mathrm{mag}}}{T'} dT'$, with T_1 being the lowest temperature of the measured data.

We measured the ac susceptibility in the frequency range between 16 Hz and 1 kHz down to 50 mK using a compensated-coil susceptometer and a lock-in amplifier. For the measurement of the static magnetization, we used a SQUID magnetometer in a commercial setup and another one in a self-built setup operated in a dilution refrigerator. Furthermore, we used InSb-GaAs Hall sensors, which allowed us to gather data in the wide temperature range between 50 mK and 300 K (here, only data up to 20 K are shown) and fields up to 5 T. In all experiments, we applied the magnetic field along the [111] direction, for which one spin per tetrahedron is parallel to the external field.

III. RESULTS

We present our specific-heat data of $Ho_2Ti_2O_7$ and $Pr_2Hf_2O_7$ in Fig. 1(a) together with literature data for $Dy_2Ti_2O_7$ from Ramirez *et al.* [3]. For $Ho_2Ti_2O_7$, previous specific-heat data are only available for temperatures above about 0.8 K [20] and above 0.5 K [21]. These data agree nicely with our specific-heat results at these higher temperatures. For $Pr_2Hf_2O_7$, we are not aware of any previous specific-heat data.

For both, $Ho_2Ti_2O_7$ and $Pr_2Hf_2O_7$, two features appear in the specific heat: a broad maximum or shoulder at about 2 K, as well as a larger and sharper anomaly at about 0.5 K ($Ho_2Ti_2O_7$) respectively at about 0.1 K ($Pr_2Hf_2O_7$). While the two anomalies merge in $Ho_2Ti_2O_7$, they are clearly separated in $Pr_2Hf_2O_7$. The literature data on $Dy_2Ti_2O_7$ [3], shown in Fig. 1(a), do not reflect any additional anomaly towards low temperatures and are in line with specific-heat results obtained by Giblin *et al.* measured for isotope-pure $^{162}Dy_2Ti_2O_7$ [22].

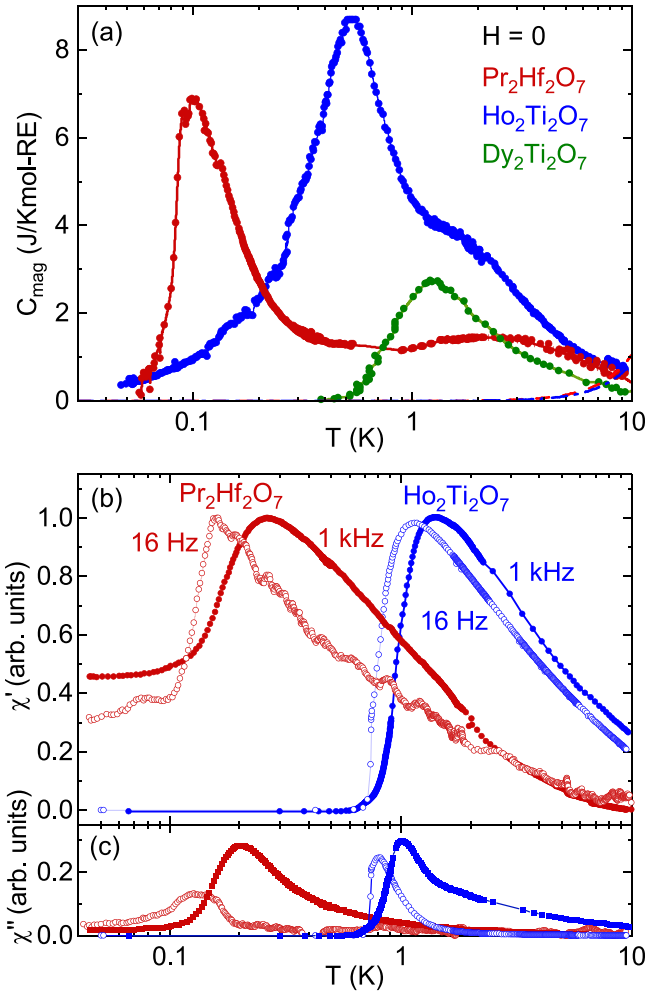

FIG. 1. (a) Low-temperature specific heat of $Pr_2Hf_2O_7$ and $Ho_2Ti_2O_7$ as function of temperature, compared to literature data for $Dy_2Ti_2O_7$ [3], all scaled in mol per rare-earth atom. Dashed lines of corresponding color show the subtracted phonon background estimated from data up to 40 K. Real (b) and imaginary part (c) of the zero-field dynamic magnetic susceptibility of $Pr_2Hf_2O_7$ and $Ho_2Ti_2O_7$ as function of temperature.

The ac susceptibility shows pronounced peaks in its real [Fig. 1(b)] as well as in its imaginary part [Fig. 1(c)]. These peaks appear for $Ho_2Ti_2O_7$ at roughly the same temperature range as the shoulder in the specific heat. For $Pr_2Hf_2O_7$, the peaks lie close to the low-temperature maximum in the specific heat, especially at low excitation frequency. While the shift of the maxima with frequency in both compounds is typical for spin-glass and spin-liquid materials [23], the ac-susceptibility signals do not show the usually observed behavior. In particular, for $Pr_2Hf_2O_7$, the real part of the ac susceptibility does not vanish down to lowest temperature. For $Ho_2Ti_2O_7$, we observe on the contrary that the ac susceptibility, both real and imaginary parts, sharply drop to zero below about 0.7 K. These observations advocate for nontrivial physics beyond the spin-ice model in the magnetic systems of both compounds.

TABLE I. Nuclear magnetic properties of ^{141}Pr, ^{165}Ho, and the five most abundant Dy isotopes [30]. I is the total nuclear spin quantum number, μ_n the nuclear magnetic moment in units of the nuclear magneton μ_N, and Q the nuclear quadrupolar moment.

Isotope	Abundance (%)	I	μ_n (μ_N)	Q (fm^2)
^{141}Pr	100	5/2	4.28	−7.7
^{160}Dy	2	0	0	0
^{161}Dy	19	5/2	−0.48	247.7
^{162}Dy	25	0	0	0
^{163}Dy	24	5/2	0.67	265.0
^{164}Dy	28	0	0	0
^{165}Ho	100	7/2	4.18	358.0

The shoulder at about 1.5 K in the specific heat of $Ho_2Ti_2O_7$ as well as the broad maximum around 3 K in $Pr_2Hf_2O_7$ originate in the excitation of three-in-one-out and one-in-three-out spin configurations on the rare-earth corner-sharing tetrahedra and, thus, with the emergence of magnetic monopole excitations out of the two-in-two-out state [19,24–26]. Compared to the prototypical spin-ice material $Dy_2Ti_2O_7$, the maximum in $Pr_2Hf_2O_7$ of 1.55 J/(Kmol Pr) is roughly only half as large and significantly broader than suggested by the spin-ice model [Fig. 1(a)]. This difference may occur due to non-Ising-like interactions that are present in Pr-based pyrochlores [11]. A possible additional low-temperature contribution that is linear [27] or cubic [28] in nature, predicted by quantum spin-ice models, is masked by the large low-temperature anomaly here.

While the specific-heat anomalies between 1 and 3 K are associated with the spin-ice physics, the large peaks appearing at lower temperatures cannot be described by such a scenario. In earlier reports, the authors claimed that the onset of the low-temperature anomaly in $Ho_2Ti_2O_7$ might be attributed to the high-temperature Schottky-like tail of nuclear magnetic contributions [21,25]. This was based on a simple Schottky-anomaly analysis in zero field of Blöte *et al.* for another Ho-containing pyrochlore material with nuclear $I = 7/2$ spins and large hyperfine interaction [29].

Notably, in contrast to $Ho_2Ti_2O_7$ and $Pr_2Hf_2O_7$, $Dy_2Ti_2O_7$ shows only one anomaly near 1 K and C_{mag} drops to zero below 0.5 K, as shown in Fig. 1(a). In comparison to ^{141}Pr and ^{165}Ho, natural abundant Dy has a wide distribution of isotopes, some of which carry a nuclear spin, $I = 5/2$ (Table I), but their corresponding nuclear magnetic moment is roughly an order of magnitude smaller. For these reasons, the associated temperature scale for nuclear magnetic contributions in $Dy_2Ti_2O_7$ and their impact on the physical properties are expected to be substantially lower and might contribute to the specific heat at much lower temperatures in the sub-millikelvin regime.

Figure 2 shows the magnetic specific heat, measured in various applied magnetic fields, together with the calculated entropy for both compounds. For $Ho_2Ti_2O_7$ in zero field, the entropy amounts to about $2R$ in the investigated temperature range, 0.05 to 20 K [Fig. 2(c)]. This entropy is much larger than what is expected for a pseudospin-1/2 ground-state doublet, $R\ \ln(2) = 0.693R$.

With increasing field, we observe a clear suppression of the low-temperature peak at 0.5 K of $Ho_2Ti_2O_7$ and a shift of the shoulder at about 1.5 K to higher temperatures, thereby evolving into a separate peak [Fig. 2(a)]. At 1 T, the entropy is enhanced reaching about $2.4R$ at 10 K [Fig. 2(c)]. Increasing the field further reduces the entropy again. This suppression

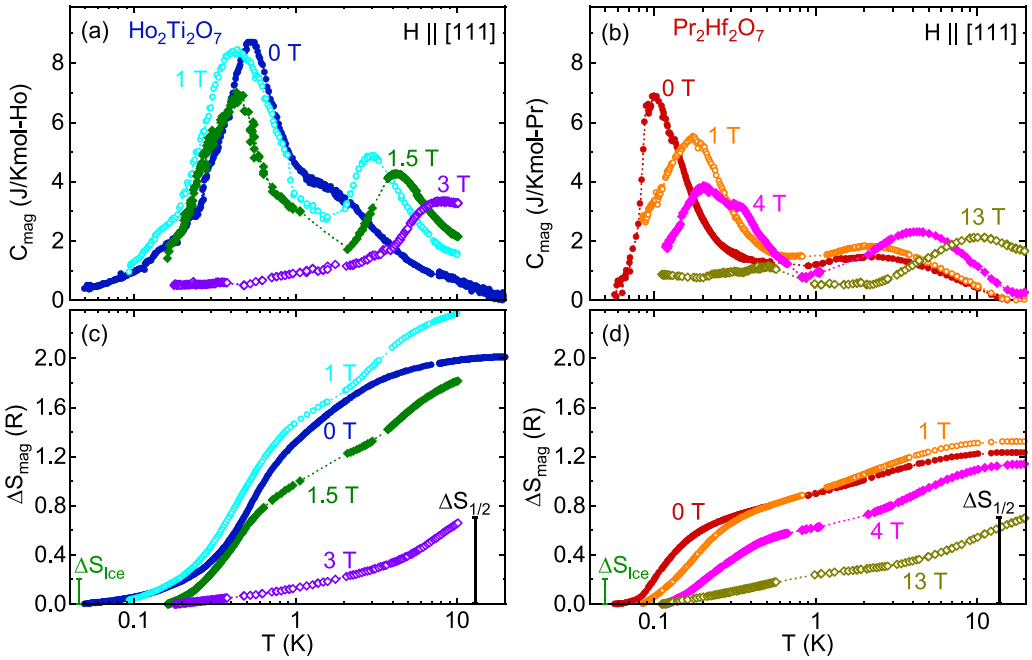

FIG. 2. Temperature-dependent magnetic part of the specific heat of (a) $Ho_2Ti_2O_7$ and (b) $Pr_2Hf_2O_7$ measured in several external magnetic fields. Entropy change as function of temperature for (c) $Ho_2Ti_2O_7$ and (d) $Pr_2Hf_2O_7$. $\Delta S_{1/2} = R\ \ln(2)$, expected for a spin-1/2 system, and $\Delta S_{ice} = R/2\ \ln(3/2) \approx 0.2R$ are indicated by black and greens bars, respectively.

of the low-temperature specific-heat anomaly and associated entropy evidences a complex, magnetic-field-dependent coupling mechanism of the electronic and nuclear moments (see Discussion below).

We find similar results for $Pr_2Hf_2O_7$, though the zero-field entropy as well as the field-dependent entropy suppression [Fig. 2(d)], extracted from the measured specific heat [Fig. 2(b)], are smaller than those of $Ho_2Ti_2O_7$. This is a consequence of the smaller J and I values in ^{141}Pr resulting in a reduced magnetic moment per Pr ion ($J = 4$, $I = 5/2$) compared to the Ho ion ($J = 8$, $I = 7/2$). Still, the entropy of $Pr_2Hf_2O_7$ is much larger than the $0.693R$—the value expected for a low-lying CEF doublet state. With increasing field, the entropy up to 20 K gradually becomes smaller. The low-temperature peak in $Pr_2Hf_2O_7$ at 0.1 K shifts to higher temperatures with increasing external field while becoming monotonously smaller, unlike the low-temperature peak in $Ho_2Ti_2O_7$ at 0.5 K.

Usually, a strong evidence in support for spin-ice behavior is the detection of a remnant spin-ice ground-state entropy, $\Delta S_{\text{ice}} = R/2\ \ln(3/2) \approx 0.2R$ [3,31]. In our case, however, the entropies of $Ho_2Ti_2O_7$ and $Pr_2Hf_2O_7$ clearly exceed the value predicted by the spin-ice model and show that analyzing the saturation entropy with and without a degeneracy-lifting external magnetic field is not viable in compounds that possess a strong coupling between the nuclear and electronic spins. The large field-dependent entropy change, obviously, is due to a modification of this coupling by the external magnetic field. The always strong hyperfine coupling does not allow us to disentangle nuclear and electronic entropies and, therefore, makes the extraction of a possible residual entropy hardly possible.

IV. DISCUSSION

In the following, we argue that an enhanced nuclear magnetism [15,16], i.e., the formation of a total spin multiplet that combines electronic and nuclear momentum, explains the observed large magnetic entropy. In bare nuclear magnetic spin systems, such as LiH [32], Cu [33], and $AuIn_2$ [34], as well as in hyperfine-enhanced nuclear spin systems with an electronic CEF singlet ground state, such as the van Vleck paramagnets $^{141}PrCu_6$ [35] and $^{141}PrNi_5$ [36], hyperfine interactions play only a minor role and lead to a splitting of the electronic states in the sub-millikelvin regime. Corresponding specific-heat anomalies occur, therefore, at temperatures much lower than the regime accessed by us. On the other hand, the coupling of nuclear spin ($\vec{I}$) to nonsinglet total electronic angular momentum ($\vec{J}$) leads to the manifestation of coupled total spin states $\vec{F} = \vec{J} + \vec{I}$ [37].

In addition to the strong CEF present in our compounds, we have to consider magnetic dipolar, exchange, hyperfine, and Zeeman interactions, as well as nuclear electric quadrupolar effects in the total spin Hamiltonian, as described by

$$\hat{H} = \hat{H}_{CEF} + \hat{H}_{DSI} + \underbrace{g_J \mu_B (\mu_0 \vec{H} \cdot \vec{J})}_{\text{electronic Zeeman}} + \underbrace{A_{HF}(\vec{I} \cdot \vec{J})}_{\text{hyperfine}} + \underbrace{g_N \mu_N (\mu_0 \vec{H} \cdot \vec{I})}_{\text{nuclear Zeeman}} + \underbrace{\frac{eQ \cdot V_{CEF}}{4I(2I-1)}\left[3m_I^2 - I(I+1)\right]}_{\text{nuclear electric quadrupolar}}. \tag{1}$$

In this equation, $\hat{H}_{CEF}$ describes the influence of the crystal-electric field and $\hat{H}_{DSI}$ the effective exchange and dipole-dipole interactions as stated in the dipolar spin-ice model [31]. The next terms describe the electronic and nuclear Zeeman effect, the hyperfine coupling of the electronic to the nuclear degrees of freedom, and the nuclear quadrupolar interaction with the gradient of the CEF. Thereby, g_J stands for the electronic Landé factor, μ_B is the Bohr magneton, A_{HF} the hyperfine coupling, g_N the nuclear g factor, e the elementary charge, V_{CEF} the CEF potential, and m_I the nuclear magnetic quantum number.

In the strongly hyperfine-interacting nuclei ^{141}Pr and ^{165}Ho in $Pr_2Hf_2O_7$ and $Ho_2Ti_2O_7$, respectively, F multiplets with nonequidistant energy splitting replace the electronic CEF ground-state doublets [37]. A simplified single-ion model that ignores spin-spin interactions with the neighboring ions is sketched in Fig. 3. The nature of the coupling and, thereby, the positions of the multiplet levels depend on the magnetic field at the ion site. On the left side of Fig. 3, the magnetic field is small against the interaction strength and $\vec{J}$ and $\vec{I}$ are coupled to a total angular momentum $\vec{F}$, whose possible states are described by the total quantum number F and the magnetic quantum number m_F. On the right side of Fig. 3, in the regime of stronger fields, $\vec{J}$ and $\vec{I}$ decouple leading to the usually considered CEF-split electronic states that are further split to equidistant hyperfine states. Here, the resulting states are described by the independent magnetic quantum numbers m_J and m_I.

The magnitude of the hyperfine split can be estimated by $a = g_N \mu_N (1 + K) B_J / \sqrt{J(J+1)}$, with B_J being the internal electronic magnetic field at the site of the nucleus and K a parameter that describes the electron-nuclear interaction, known as Knight shift in metals [37].

With this model, we can compute the partition function

$$Z(T) = \sum_i \exp\left(\frac{-\Delta_i}{k_B T}\right), \tag{2}$$

with Δ_i the energies of the excited levels with respect to the ground state and k_B the Boltzmann constant. From that, we obtain thermodynamic properties such as the specific heat

$$C = \frac{\partial^2}{\partial T^2}(k_B T\ \ln Z). \tag{3}$$

The calculated temperature-dependent zero-field specific heats of $Pr_2Hf_2O_7$ and $Ho_2Ti_2O_7$ capture the key features of our experimental data (Fig. 4). The quantitative deviations between the measured and calculated specific heat might originate from interatomic and quadrupolar interactions. These influences are obviously not captured by a single-ion model, but they certainly modify the multiplet. In turn, this alters the position of the peaks in the specific heat on the temperature axis, since these peaks are proportional to Δ_i. Nevertheless, the appearance of the calculated anomalies in the experimental data do advocate for a complex energy-level scheme generated by the enhanced hyperfine coupling, while it shows at the same time that the single-ion approach is too simplistic for quantitative predictions.

We should add that, at very low temperatures, we also cannot exclude that our heat-pulse method might not be able

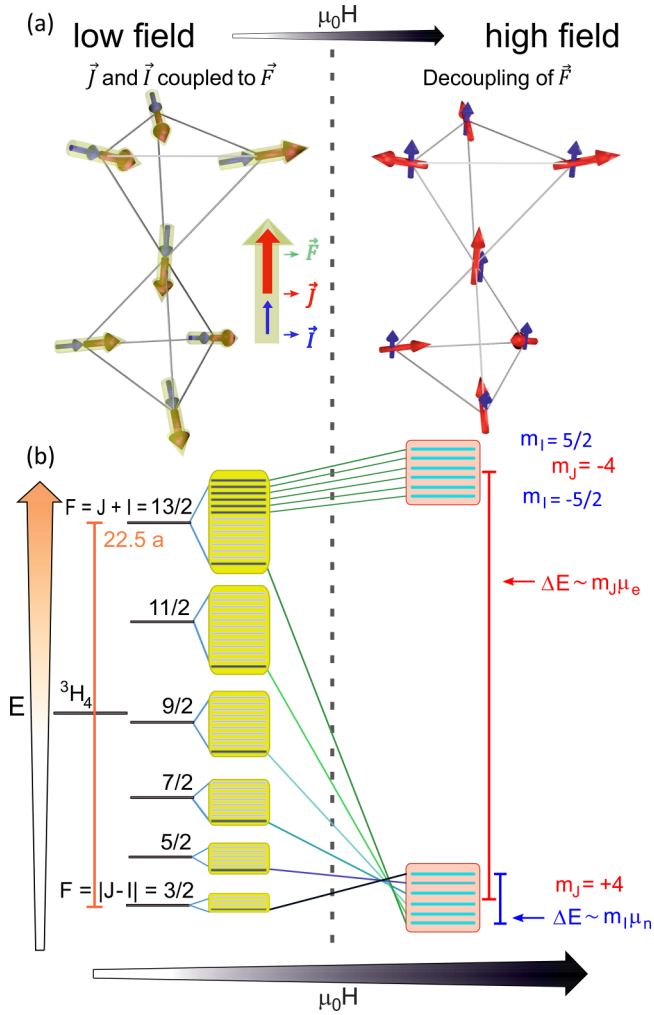

FIG. 3. (a) Scheme of the effective localized magnetic moments for the case of $Pr_2Hf_2O_7$ (for $Ho_2Ti_2O_7$ analogous, with a hyperfine split of 59.5a). In weak magnetic fields (left), the localized electronic magnetic moment, $\vec{J}$, and the nuclear spin, $\vec{I}$, couple to the total angular momentum, $\vec{F} = \vec{J} + \vec{I}$. At high fields (right), $\vec{J}$ and $\vec{I}$ decouple. (b) Simplified level scheme of the Pr^{3+} ion. In low fields (left), the multiplet is described by (F, m_F). At high fields (right), $\vec{J}$ and $\vec{I}$ decouple to a split electronic ground-state doublet with maximum m_J, whose two states are further split in $2m_I + 1$ equidistant hyperfine states [37]. Levels with $m_J \neq \pm J$ are shifted to higher energies by the CEF. (See text for further details.)

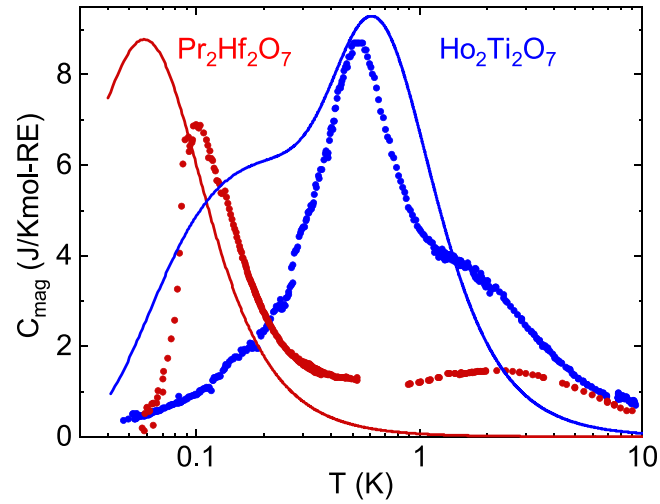

FIG. 4. Comparison of the measured (red/blue circles) specific heat of $Ho_2Ti_2O_7$ and $Pr_2Hf_2O_7$ at zero field with the calculated (red/blue line) results using the single-ion F multiplet model shown in Fig. 3 and Eq. (3). The hyperfine constants are set to $a^{Pr} = 10$ mK for the Pr and to $a^{Ho} = 42$ mK for the Ho compound.

to capture the whole nuclear specific heat. The nuclear spin-lattice relaxation time might be longer than our heat-pulse relaxation time. This might explain in particular the rapid drop of C_{mag} in $Pr_2Hf_2O_7$ below 100 mK (Fig. 4).

Nevertheless, our results clearly show that the nuclear magnetic moments are strongly intertwined with the electronic ones and contribute to the thermodynamic properties considerably. Interatomic interactions among these F states with the CEF may lead to spin structures beyond the two-in-two-out ground state or excited three-in-one-out configurations, because additional levels will increase transverse interactions perpendicular to the local Ising axis. Such transverse interactions are predicted to essentially modify the spin-ice physics [7,8,27]. Another consequence of these strongly hyperfine-coupled states might be the faster relaxation of magnetic perturbations of the two-in-two-out state in $Ho_2Ti_2O_7$ compared to $Dy_2Ti_2O_7$, as reported in Ref. [38], due to its increased number of available states in the relevant temperature range.

The specific heat and entropy get strongly suppressed when applying magnetic fields (Fig. 2). This can be understood qualitatively by a strong field-induced shift and crossing of the F levels and, in particular, by a decoupling of $\vec{F}$ into nearly independent moments $\vec{J}$ and $\vec{I}$ at higher fields of a few tesla, as sketched on the right side of Fig. 3.

In the high-field limit, i.e., for the Paschen-Back scenario [37], the nuclear spin and the electronic total angular momentum decouple and form a wide-split ground-state doublet, whose two $m_J = \pm J$ states are further split into $2m_I + 1$ equidistant hyperfine states [37]. States with other m_J are shifted by CEF effects to high energies and can only be populated at temperatures above about 100 K [10,12]. The hyperfine splitting of each m_J state, $\Delta E \propto m_I \mu_n$. is of the order 150 μK in an external magnetic field of 1 T. Above 50 mK, the lowest temperature attained in our specific-heat measurements, all m_I states are equally occupied and, therefore, do not contribute to the specific heat anymore. Consequently, C_{mag} and the corresponding entropy are strongly reduced at high fields in our experimental temperature window. The bare hyperfine contribution would appear only at much lower temperatures in the specific heat. For $Ho_2Ti_2O_7$ at 3 T and for $Pr_2Hf_2O_7$ at 13 T, we observe an entropy change which approaches the one expected for an Ising-like spin-1/2 system.

While the nuclear and electronic moments are decoupled at strong fields, a description of the thermodynamic properties, including the specific heat, in intermediate applied magnetic fields is highly challenging, even on a qualitative level. For intermediate magnetic fields, the energy-level scheme becomes very complex. Even the single-ion hyperfine interaction model has no simple solution here [37].

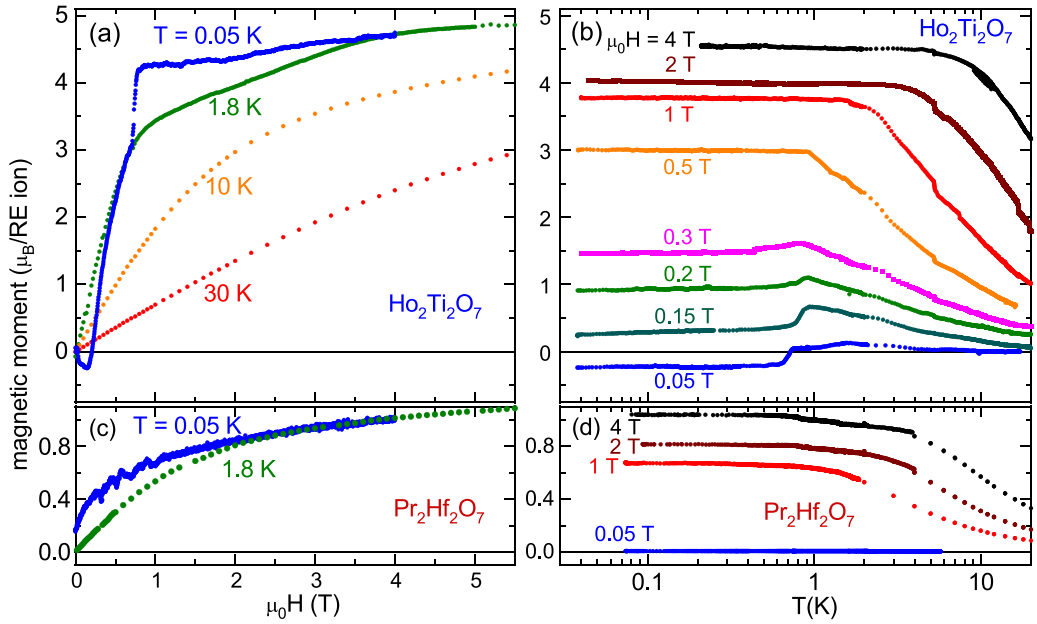

FIG. 5. Magnetization of $Ho_2Ti_2O_7$ as function of (a) magnetic field and (b) temperature. At small fields and low temperatures, the magnetic moment is negative. Panels (c) and (d) show the magnetization of $Pr_2Hf_2O_7$ as function of field and temperature, respectively. The saturation value at 4 T, about $1.0\mu_B$, is slightly smaller than the expected magnetic moment per Pr ion for a two-in-two-out spin configuration of the pyrochlore lattice and we observe no sign for a transition into a kagome-ice phase as indicated around 0.5 T in the $Ho_2Ti_2O_7$ data at $T = 0.05$ K shown in (a).

The existence of nuclear magnetic anomalies in the specific heat at rather high temperatures has consequences for the spin-ice physics. To fully understand the physics of correlated spins in spin-ice materials with a considerable nuclear magnetic moment, a detailed theoretical model that encompasses electron-nuclear interactions is necessary. This model needs to include on-site hyperfine and quadrupolar interactions as well as interactions with the neighboring ions which goes beyond the scope of the present paper.

The complex term schemes of the hyperfine-enhanced-coupled ions may also explain the field-dependent magnetization of $Ho_2Ti_2O_7$ at very low temperatures, shown in Figs. 5(a) and 5(b). As known from previous reports [14,39], $Ho_2Ti_2O_7$ shows the expected Ising-limit magnetization at moderate fields and temperatures in the kelvin range, corresponding to about $5\mu_B$, i.e., 1/2 of the full Ho moment. Only at much larger magnetic fields (above about 25 T), higher CEF levels get occupied leading to a gradually increasing magnetization. However, even 120 T are not sufficient to reach full saturation [14]. Similar to the case of $Dy_2Ti_2O_7$ [4], a kagome-ice-like plateau with 1/3 of the full Ho moment evolves at about 0.7 T for fields aligned along the [111] direction in $Ho_2Ti_2O_7$ [see Ref. [14] and Fig. 5(a)].

Our magnetization measurements at very low temperatures (50 mK) using the mentioned SQUID magnetometer and Hall sensor reveal an unusual negative magnetization in small applied fields, for zero-field cooling [Fig. 5(a)]. In a field of 0.05 T, the negative magnetization (about $-0.23\mu_B$) is temperature independent, until, with rising temperature, at about 0.7 K the magnetization increases by about $0.3\mu_B$ to positive values [Fig. 5(b)]. Such increasing magnetization appears at higher magnetic fields as well, up to 0.3 T. This suggests that $Ho_2Ti_2O_7$ might undergo a transition into a magnetically ordered state at very low temperatures and low fields, possibly induced by interatomic and nuclear hyperfine interactions.

It is worth noting that, in a previous study, we too have observed a negative magnetization of $0.6\mu_B$ together with an inverse hysteresis in the antiferromagnet $Nd_2Hf_2O_7$ [6]. While in small external fields, except for domain walls, the magnetization is zero in antiferromagnetic $Nd_2Hf_2O_7$, this is not the case for $Ho_2Ti_2O_7$, for which the effective interaction is ferromagnetic [9]. This suggests that the negative magnetization in $Ho_2Ti_2O_7$ is a bulk phenomenon. A speculative cause for this peculiar state may be associated with the large quadrupolar moment of the ^{165}Ho nucleus, which is interacting with the electric-field gradient generated by the O^{2-} ions.

This is further substantiated by the fact that $Pr_2Hf_2O_7$ does not show any signs for a negative magnetization [Figs. 5(c) and 5(d)]. Indeed, ^{141}Pr has a nuclear magnetic moment of similar magnitude as of ^{165}Ho, but a quadrupolar moment that is approximately 45 times smaller (Table I).

The magnetic moment of $Pr_2Hf_2O_7$ saturates slightly above $1\mu_B$ at low temperatures and a few tesla. This is somewhat smaller than expected for the polarized three-in-one-out state projected on the [111] direction. For that, a saturation magnetization of $\mu_{sat}/2 = 1.6\mu_B$ and for a kagome-ice state $\mu_{sat}/3 = 1.1\mu_B$ is expected. This smaller saturation magnetization hints at fluctuations of the moment that are of nonthermal origin, supporting the applicability of the quantum spin-ice model for $Pr_2Hf_2O_7$.

These fluctuations are also expected to leave their mark in dynamical magnetic properties [27,40]. This has, for example, been observed in $Pr_2Sn_2O_7$ in the form of persisting spin dynamics down to lowest temperatures by measuring the spin-relaxation time with neutron diffraction [41]. The

spin dynamics are likewise reflected in the response of the sample to an oscillating external magnetic field. In line with that, the ac susceptibility of $Pr_2Hf_2O_7$ does not vanish down to lowest temperatures [see Fig. 1(b)]. Different from, for instance, $Dy_2Ti_2O_7$ [42], the spins of $Pr_2Hf_2O_7$ can be canted by the driving field and, thus, generate an ac signal. Together with the smaller saturation magnetization this corroborates the existence of nonthermal fluctuations influencing the low-temperature behavior of $Pr_2Hf_2O_7$.

V. CONCLUSION

In summary, our thermodynamic investigations clearly reveal that in $Ho_2Ti_2O_7$ and $Pr_2Hf_2O_7$ the nuclear spin and total electronic angular momentum are coupled and create a complex F-state term scheme. This makes a reliable determination of a possible residual entropy in these materials hardly possible. The strongly enhanced hyperfine coupling and possible interatomic interactions may cause cooperative phenomena, such as the unusual negative magnetization in $Ho_2Ti_2O_7$. They further may play a role in the peculiar spin dynamics of the quantum spin-liquid candidate $Pr_2Hf_2O_7$ that persists down to lowest temperatures as shown by our ac-susceptibility data. For a comprehensive understanding of the physics of pyrochlore compounds with large nuclear magnetic moments, it is, therefore, important to take such hyperfine couplings into account, as well as higher-order effects caused by the nuclear quadrupolar moment.

ACKNOWLEDGMENTS

We acknowledge support from the Deutsche Forschungsgemeinschaft (DFG) through SFB 1143 (Project No. 247310070), GRK 1621, and the Würzburg-Dresden Cluster of Excellence on Complexity and Topology in Quantum Matter *ct.qmat* (EXC 2147, Project No. 390858490), as well as the support of the HLD at HZDR, member of the European Magnetic Field Laboratory (EMFL). The crystals of $Pr_2Hf_2O_7$ were synthesized at the Core Lab Quantum Materials, at Helmholtz Zentrum Berlin für Materialien und Energie (HZB), Germany. We also thank J. Hornung and L. Opherden for feedback and helpful discussions.

[1] L. Balents, Nature (London) **464**, 199 (2010).
[2] S. T. Bramwell and M. J. Harris, J. Phys.: Condens. Matter **32**, 374010 (2020).
[3] A. P. Ramirez, A. Hayashi, R. J. Cava, R. Siddharthan, and B. S. Shastry, Nature (London) **399**, 333 (1999).
[4] Z. Hiroi, K. Matsuhira, S. Takagi, T. Tayama, and T. Sakakibara, J. Phys. Soc. Jpn. **72**, 411 (2003).
[5] C. Castelnovo, R. Moessner, and S. L. Sondhi, Nature (London) **451**, 42 (2008).
[6] L. Opherden, T. Bilitewski, J. Hornung, T. Herrmannsdörfer, A. Samartzis, A. T. M. N. Islam, V. K. Anand, B. Lake, R. Moessner, and J. Wosnitza, Phys. Rev. B **98**, 180403(R) (2018).
[7] M. J. P. Gingras and P. A. McClarty, Rep. Prog. Phys. **77**, 056501 (2014).
[8] B. C. den Hertog and M. J. P. Gingras, Phys. Rev. Lett. **84**, 3430 (2000).
[9] J. S. Gardner, M. J. P. Gingras, and J. E. Greedan, Rev. Mod. Phys. **82**, 53 (2010).
[10] S. Rosenkranz, A. P. Ramirez, A. Hayashi, R. J. Cava, R. Siddharthan, and B. S. Shastry, J. Appl. Phys. **87**, 5914 (2000).
[11] A. J. Princep, D. Prabhakaran, A. T. Boothroyd, and D. T. Adroja, Phys. Rev. B **88**, 104421 (2013).
[12] R. Sibille, E. Lhotel, M. C. Hatnean, G. Balakrishnan, B. Fak, N. Gauthier, T. Fennell, and M. Kenzelmann, Phys. Rev. B **94**, 024436 (2016).
[13] D. Pomaranski, L. R. Yaraskavitch, S. Meng, K. A. Ross, H. M. L. Noad, H. A. Dabkowska, B. D. Gaulin, and J. B. Kycia, Nat. Phys. **9**, 353 (2013).
[14] L. Opherden, T. Herrmannsdörfer, M. Uhlarz, D. I. Gorbunov, A. Miyata, O. Portugall, I. Ishii, T. Suzuki, H. Kaneko, H. Suzuki, and J. Wosnitza, Phys. Rev. B **99**, 085132 (2019).
[15] B. Bleaney, J. Appl. Phys. **34**, 1024 (1963).
[16] B. Bleaney, Physica **69**, 317 (1973).
[17] D. E. MacLaughlin, Y. Ohta, Y. Machida, S. Nakatsuji, G. M. Luke, K. Ishida, R. H. Heffner, L. Shu, and O. O. Bernal, Phys. B: Condens. Matter **404**, 667 (2009).
[18] F. R. Foronda, F. Lang, J. S. Möller, T. Lancaster, A. T. Boothroyd, F. L. Pratt, S. R. Giblin, D. Prabhakaran, and S. J. Blundell, Phys. Rev. Lett. **114**, 017602 (2015).
[19] V. K. Anand, L. Opherden, J. Xu, D. T. Adroja, A. T. M. N. Islam, T. Herrmannsdörfer, J. Hornung, R. Schönemann, M. Uhlarz, H. C. Walker, N. Casati, and B. Lake, Phys. Rev. B **94**, 144415 (2016).
[20] R. Siddharthan, B. S. Shastry, A. P. Ramirez, A. Hayashi, R. J. Cava, and S. Rosenkranz, Phys. Rev. Lett. **83**, 1854 (1999).
[21] S. T. Bramwell, M. J. Harris, B. C. den Hertog, M. J. P. Gingras, J. S. Gardner, D. F. McMorrow, A. R. Wildes, A. L. Cornelius, J. D. M. Champion, R. G. Melko, and T. Fennell, Phys. Rev. Lett. **87**, 047205 (2001).
[22] S. R. Giblin, M. Twengström, L. Bovo, M. Ruminy, M. Bartkowiak, P. Manuel, J. C. Andresen, D. Prabhakaran, G. Balakrishnan, E. Pomjakushina, C. Paulsen, E. Lhotel, L. Keller, M. Frontzek, S. C. Capelli, O. Zaharko, P. A. McClarty, S. T. Bramwell, P. Henelius, and T. Fennell, Phys. Rev. Lett. **121**, 067202 (2018).
[23] J. A. Mydosh, *Spin Glasses: An Experimental Introduction* (CRC Press, London, 1993).
[24] R. Higashinaka, H. Fukazawa, D. Yanagishima, and Y. Maeno, J. Phys. Chem. Solids **63**, 1043 (2002).
[25] R. G. Melko and M. J. P. Gingras, J. Phys.: Condens. Matter **16**, R1277 (2004).
[26] R. Sibille, N. Gauthier, H. Yan, M. Ciomaga Hatnean, J. Ollivier, B. Winn, U. Filges, G. Balakrishnan, M. Kenzelmann, N. Shannon, and T. Fennell, Nat. Phys. **14**, 711 (2018).
[27] P. A. Lee, Science **321**, 1306 (2008).
[28] M. Hermele, M. P. A. Fisher, and L. Balents, Phys. Rev. B **69**, 064404 (2004).
[29] H. W. J. Blöte, R. F. Wielinga, and W. J. Huiskamp, Physica **43**, 549 (1969).
[30] *CRC Handbook of Chemistry and Physics*, edited by J. Rumble (CRC Press, Boca Raton, 2022).

[31] S. T. Bramwell and M. J. P. Gingras, Science **294**, 1495 (2001).
[32] Y. Roinel, V. Bouffard, G. L. Bacchella, M. Pinot, P. Mériel, P. Roubeau, O. Avenel, M. Goldman, and A. Abragam, Phys. Rev. Lett. **41**, 1572 (1978).
[33] P. J. Hakonen, S. Yin, and O. V. Lounasmaa, Phys. Rev. Lett. **64**, 2707 (1990).
[34] T. Herrmannsdörfer, P. Smeibidl, B. Schröder-Smeibidl, and F. Pobell, Phys. Rev. Lett. **74**, 1665 (1995).
[35] J. Babcock, J. Kiely, T. Manley, and W. Weyhmann, Phys. Rev. Lett. **43**, 380 (1979).
[36] M. Kubota, H. R. Folle, C. Buchal, R. M. Mueller, and F. Pobell, Phys. Rev. Lett. **45**, 1812 (1980).
[37] H. Haken and H. C. Wolf, *The Physics of Atoms and Quanta* (Springer-Verlag, Berlin, Heidelberg, 2005).
[38] C. Paulsen, S. R. Giblin, E. Lhotel, D. Prabhakaran, K. Matsuhira, G. Balakrishnan, and S. T. Bramwell, Nat. Commun. **12**, 661 (2016).
[39] S. T. Bramwell, M. N. Field, M. J. Harris, and I. P. Parkin, J. Phys.: Condens. Matter **12**, 483 (2000).
[40] S. Onoda and Y. Tanaka, Phys. Rev. B **83**, 094411 (2011).
[41] H. D. Zhou, C. R. Wiebe, J. A. Janik, L. Balicas, Y. J. Yo, Y. Qiu, J. R. D. Copley, and J. S. Gardner, Phys. Rev. Lett. **101**, 227204 (2008).
[42] J. Snyder, B. G. Ueland, J. S. Slusky, H. Karunadasa, R. J. Cava, and P. Schiffer, Phys. Rev. B **69**, 064414 (2004).